Using the CloudSat data over precipitation systems to help constrain the GPM retrieval algorithms

Z.S. Haddad[1], F.J. Turk[1] and K.-W Park[1,2]
[1]Jet Propulsion Laboratory, California Institute of Technology, Pasadena CA 91109-8099
[2]APEC Climate Center, 1463 U-dong Haeundae-gu, Busan 612-020, Korea

Original motivation: perform combined retrievals of TRMM and CloudSat instantaneous measurements

Approach: perform joint radar retrievals from the surface up, then forward compare with the radiometers

Problem: 94-GHz attenuation slope below the melting layer, in rain, rarely decreases at a rate consistent with forward predictions from Mie scattering calculations applied to sampled DSDs.

New motivations:
1) Understand the multiple scattering (i.e. learn how to detect, quantify and mitigate it)
2) Use global intersection data set to generate global database of realistic forward simulations

Example:

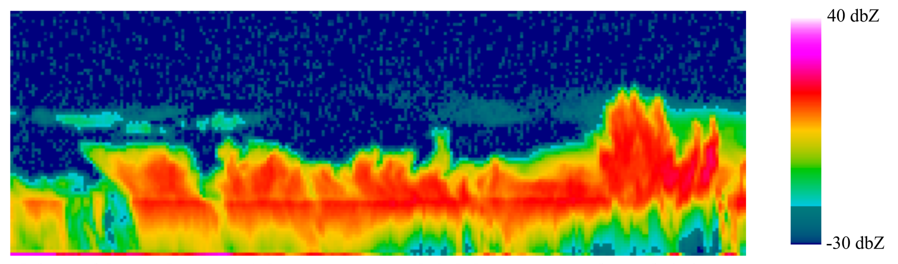

CloudSat CPR, 12 January 2009, around Tahiti

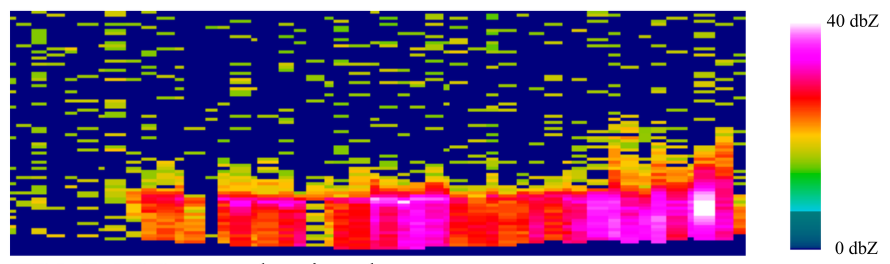

TRMM PR, nearly simultaneous

We first constructed a database of 40,497 DSD profiles synthesized from TRMM retrievals augmented with pre-specified profiles of $D_m/R^{0.155}$ (D_m= mass-weighted mean drop diameter, R=rain rate; we injected 60 profiles of $D_m/R^{0.155}$ for every TRMM-retrieved rain rate profile, retaining only those whose resulting values of $D_m/R^{0.155}$ remained between 0.35mm and 3.5mm)

For each of these profiles, we forward-calculated the single-scatter 94 GHz profiles.
For the multiple-scattering study, we then retained sub-profiles consisting of 21-coordinate vectors with
9 Z_{14} (from 3625m down to 1625m), i.e. ignoring bottom 5 bins, followed by
11 ΔZ_{94} (from "3625m minus 3375m" down to "1125m minus 825m") – so ignoring bottom 3 bins,

$$\begin{pmatrix} Z_{14}|_{3625m} \\ Z_{14}|_{3375m} \\ Z_{14}|_{3125m} \\ Z_{14}|_{2875m} \\ Z_{14}|_{2625m} \\ Z_{14}|_{2375m} \\ Z_{14}|_{2125m} \\ Z_{14}|_{1875m} \\ Z_{14}|_{1625m} \\ Z_{94}|_{3625m} - Z_{94}|_{3375m} \\ Z_{94}|_{3375m} - Z_{94}|_{3125m} \\ Z_{94}|_{3125m} - Z_{94}|_{2875m} \\ Z_{94}|_{2875m} - Z_{94}|_{2635m} \\ Z_{94}|_{2635m} - Z_{94}|_{2375m} \\ Z_{94}|_{2375m} - Z_{94}|_{2125m} \\ Z_{94}|_{2125m} - Z_{94}|_{1875m} \\ Z_{94}|_{1875m} - Z_{94}|_{1625m} \\ Z_{94}|_{1625m} - Z_{94}|_{1375m} \\ Z_{94}|_{1375m} - Z_{94}|_{1125m} \\ Z_{94}|_{1125m} - Z_{94}|_{875m} \end{pmatrix}^{(1)} \cdots \begin{pmatrix} Z_{14}|_{3625m} \\ Z_{14}|_{3375m} \\ Z_{14}|_{3125m} \\ Z_{14}|_{2875m} \\ Z_{14}|_{2625m} \\ Z_{14}|_{2375m} \\ Z_{14}|_{2125m} \\ Z_{14}|_{1875m} \\ Z_{14}|_{1625m} \\ Z_{94}|_{3625m} - Z_{94}|_{3375m} \\ Z_{94}|_{3375m} - Z_{94}|_{3125m} \\ Z_{94}|_{3125m} - Z_{94}|_{2875m} \\ Z_{94}|_{2875m} - Z_{94}|_{2635m} \\ Z_{94}|_{2635m} - Z_{94}|_{2375m} \\ Z_{94}|_{2375m} - Z_{94}|_{2125m} \\ Z_{94}|_{2125m} - Z_{94}|_{1875m} \\ Z_{94}|_{1875m} - Z_{94}|_{1625m} \\ Z_{94}|_{1625m} - Z_{94}|_{1375m} \\ Z_{94}|_{1375m} - Z_{94}|_{1125m} \\ Z_{94}|_{1125m} - Z_{94}|_{875m} \end{pmatrix}^{(40497)}$$

on which we can perform a principal components analysis to
1) capture the modes of the vertical behavior of the Z_{94} slope (under the single-scatter assumption),
2) quantify its dependence on the values of Z_{14} and the values of the highest ΔZ_{94}
3) test when the modes of the slope of a measured profile are consistent with the empirical modes under the single-scatter assumption
4) restore the most-likely single-scatter ΔZ_{94} that should be inferred at lower altitudes from the values of ΔZ_{94} at the higher altitudes

The 20 principal components are the following columns (with their contributions to the variance at the bottom, and with their largest coefficient highlighted in bold (note that the lowest 8 principal components have their largest coefficients at ΔZ_{94}):

-3.05e-1	4.69e**-1**	**-6.35e-1**	**3.84e-1**	-2.45e-1	8.06e-3	-2.33e-1	6.58e-2	-7.15e-2	6.28e-2	-8.76e-2	-1.65e-2	-1.24e-2	3.23e-3	-1.82e-3	4.84e-3	1.17e-3	-3.21e-4	-1.76e-2	-1.38e-2
-3.24e-1	4.35e**-1**	1.38e-1	3.68e-2	3.67e-1	1.58e-1	**6.63e-1**	1.47e-1	1.47e-1	1.13e-1	-5.25e-2	-1.10e-1	4.56e-3	-3.16e-2	-4.06e-2	5.80e-2	3.17e-3	-5.99e-2	-1.29e-2	-7.15e-2
-3.16e-1	2.71e**-1**	1.21e-1	-1.73e-1	6.28e-2	-1.07e-1	-1.24e-1	-3.34e-1	6.55e-3	**-3.85e-1**	**5.30e-1**	1.73e-1	-1.90e-1	2.74e-1	2.59e-1	5.21e-3	1.58e-2	-3.31e-2	2.39e-3	-3.53e-2
-3.20e-1	1.46e**-1**	1.68e-1	-2.49e-1	-7.72e-2	-2.78e-1	-1.36e-1	-1.47e-1	1.42e-1	-3.35e-1	-4.28e-1	1.55e-1	3.90e-1	-3.02e-1	-2.50e-1	3.99e-2	7.22e-2	7.82e-2	-2.62e-3	6.50e-2
-3.39e-1	9.11e**-3**	1.64e-1	-2.90e-1	-1.83e-1	-1.99e-1	-1.16e-1	6.57e-2	-2.51e-1	3.04e-1	1.53e-1	**-6.22e-1**	-1.08e-2	-9.36e-2	-1.86e-2	-2.61e-1	-1.70e-1	8.04e-2	-6.63e-2	3.04e-2
-3.40e-1	-1.28e**-1**	1.03e-1	-2.31e-1	-2.28e-1	-3.22e-2	-4.94e-2	**5.20e-1**	1.64e-2	3.42e-1	2.66e-2	4.52e-1	-9.35e-3	1.49e-1	1.80e-1	1.85e-1	2.18e-1	3.81e-2	1.34e-1	8.96e-4
-3.42e-1	-2.55e**-1**	-3.25e-3	-1.09e-1	-2.18e-1	**6.62e-1**	-8.00e-2	-1.45e-1	2.28e-1	-9.30e-2	-5.69e-2	-5.20e-2	-2.59e-1	3.24e-2	-3.52e-1	7.87e-3	-1.16e-1	-1.17e-1	5.48e-2	-5.87e-2
-3.41e-1	-3.78e**-1**	-1.61e-1	6.93e-2	2.03e-1	6.90e-2	1.88e-1	-2.11e-1	**-5.86e-1**	-4.46e-2	-2.05e-1	1.76e-1	1.69e-1	8.39e-3	2.50e-1	-1.18e-1	-1.16e-1	-2.15e-1	-1.95e-2	2.74e-2
-3.37e-1	-4.74e**-1**	-2.17e-1	2.56e-1	**3.94e-1**	-2.92e-1	-7.64e-2	5.16e-2	4.13e-1	-2.14e-2	1.43e-1	-1.65e-1	-5.41e-2	-4.94e-2	-1.70e-2	9.72e-2	1.01e-1	2.19e-1	-8.54e-2	3.45e-2
-2.59e-2	7.36e**-2**	2.18e-1	1.48e-1	3.44e-1	2.72e-1	-3.99e-1	4.88e-1	-2.53e-1	-3.39e**-1**	4.82e-2	-9.60e-2	1.52e-2	-1.89e-1	-1.07e-2	-1.46e-1	2.19e-1	-5.19e-2	-2.23e-3	-1.93e-1
-3.22e-2	8.43e**-2**	1.65e-1	1.61e-1	2.58e-1	1.35e-1	-3.09e-1	-1.30e-1	2.00e-2	3.66e**-1**	2.32e-1	1.41e-1	**5.13e-1**	1.46e-1	-2.09e-1	1.65e-1	-3.99e-1	1.12e-2	1.29e-1	-4.63e-2
-3.96e-2	9.50e**-2**	1.67e-1	1.38e-1	1.45e-1	3.59e-2	-1.15e-1	2.89e-2	9.48e-2	2.37e-3	-2.72e-1	9.17e-2	-2.84e-1	3.81e-2	2.00e-1	-3.28e-1	-2.86e-1	2.80e-1	4.32e-1	4.87e-1
-4.38e-2	7.51e**-2**	2.00e-1	1.55e-1	7.35e-2	6.23e-2	-1.29e-1	-2.14e-1	-1.44e-1	2.42e-1	5.06e-2	-9.02e-3	-1.37e-1	-1.05e-1	-1.49e-1	2.12e-1	**4.45e-1**	-2.30e-1	-2.29e-1	**6.12e-1**
-4.55e-2	4.64e**-2**	2.29e-1	1.54e-1	-1.56e-3	-7.50e-3	-8.81e-2	-5.59e-2	5.16e-2	1.74e-1	-1.67e-1	3.05e-1	-2.18e-1	6.24e-3	2.54e-2	-2.63e-1	-1.75e-1	2.11e-1	**-7.20e-1**	-2.13e-1
-4.86e-2	1.10e**-2**	2.24e-1	1.85e-1	-7.61e-2	1.54e-1	-9.26e-2	-3.82e-1	4.06e-2	1.96e-1	-2.41e-1	-2.11e-1	7.09e-2	5.59e-2	3.65e-1	9.08e-2	4.20e-1	2.65e-1	2.17e-1	-3.78e-1
-5.08e-2	-1.44e**-2**	1.77e-1	2.26e-1	1.97e-3	-3.58e-1	4.11e-2	-6.07e-2	-3.26e-1	3.18e-2	-4.04e-2	1.10e-1	-4.61e-1	-6.01e-2	**-4.39e-1**	2.49e-1	-8.78e-2	1.01e-2	2.98e-1	-3.05e-1
-5.04e-2	-3.94e**-2**	2.19e-1	2.64e-1	-1.27e-1	-2.38e-1	-8.52e-2	4.02e-2	3.25e-1	4.19e-2	-1.12e-1	-5.92e-2	1.13e-2	6.84e-2	1.50e-1	-2.24e-1	-6.11e-2	**-7.56e-1**	8.23e-2	-1.13e-1
-5.14e-2	-4.89e**-2**	2.34e-1	2.61e-1	-2.83e-1	6.80e-2	5.44e-2	1.36e-1	-2.52e-2	-2.41e-1	1.40e-2	-1.56e-1	1.95e-2	-2.16e-1	3.48e-1	**5.72e-1**	-3.82e-1	5.34e-2	-1.50e-1	1.27e-1
-5.27e-2	-7.38e**-2**	1.80e-1	2.82e-1	-2.06e-1	-5.67e-2	1.54e-1	1.45e-1	-1.10e-1	-2.53e-1	-7.77e-2	-1.50e-1	2.19e-1	**7.02e-1**	-2.57e-1	-8.63e-2	1.19e-1	1.63e-1	-8.92e-2	1.45e-1
-5.42e-2	-9.06e**-2**	1.14e-1	3.50e-1	-3.32e-1	5.29e-2	2.68e-1	-4.56e-2	9.43e-3	-1.95e-2	4.43e**-1**	2.10e-1	1.94e-1	-4.22e-1	-8.48e-2	-3.80e-1	1.26e-1	1.52e-1	1.39e-1	3.16e-2
89.44%	6.21%	0.95%	0.88%	0.56%	0.32%	0.25%	0.19%	0.18%	0.15%	0.14%	0.14%	0.11%	0.10%	0.09%	0.08%	0.07%	0.06%	0.05%	0.04%
89.44%	95.65%	96.60%	97.48%	98.04%	98.36%	98.61%	98.80%	98.98%	99.13%	99.27%	99.41%	99.50%	99.60%	99.69%	99.77%	99.84%	99.90%	99.90%	99.99%

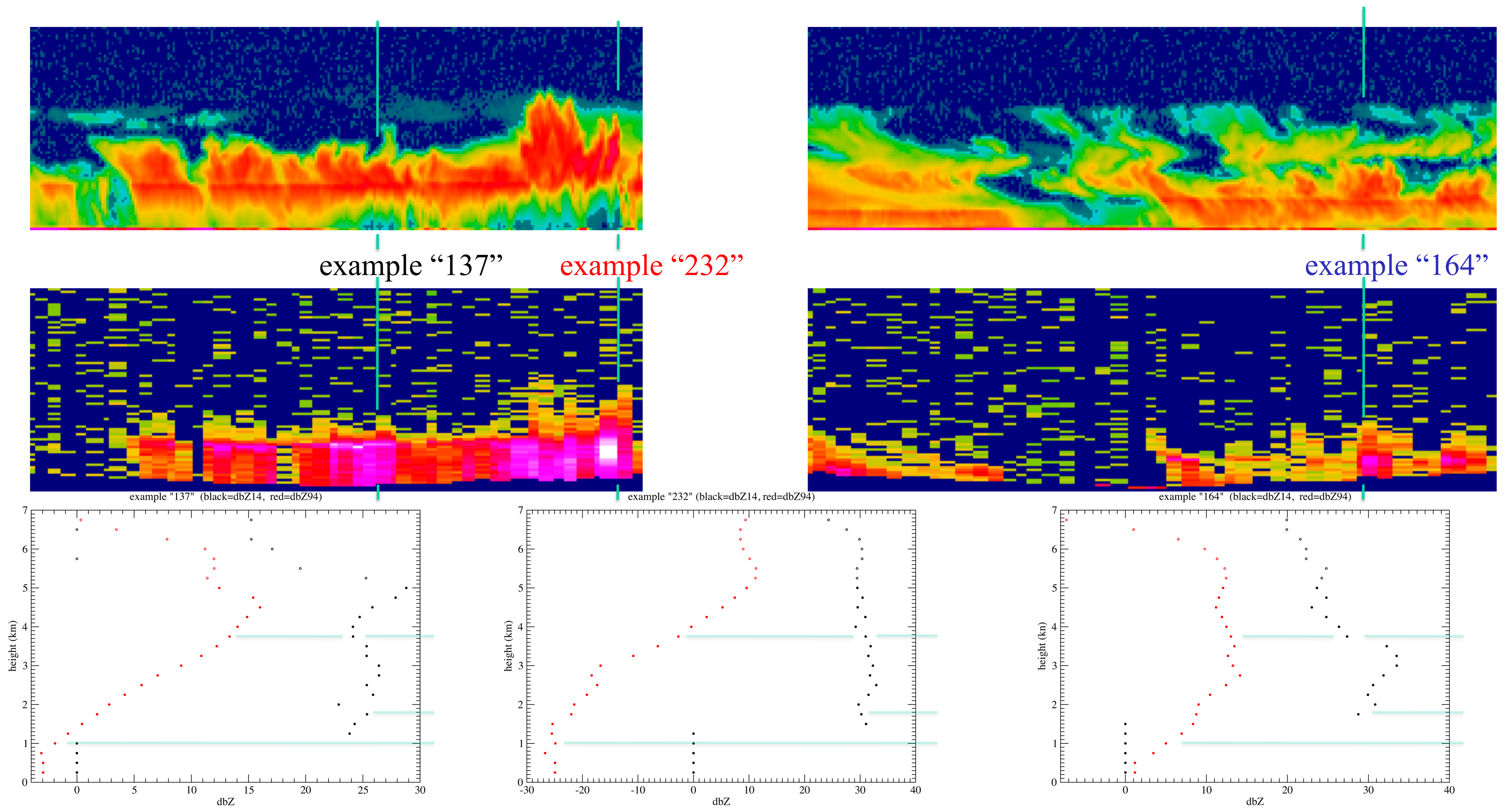

Eof14	1	-79.4	0.67
Eof14	2	3.8	0.01
Eof14	3	0.6	1.16
Eof14	4	-0.3	-0.10
Eof14	5	-2.2	-1.17
Eof14	6	0.2	-0.33
Eof14	7	1.0	-0.06
Eof14	8	-0.8	-1.03
Eof14	9	-1.4	-1.76
Eof94	1	-4.5	0.06
Eof94	2	1.2	1.05
Eof94	3	0.3	-0.04
Eof94	4	-0.1	-0.25
Eof94	5	-0.1	-0.20
Eof94	6	0.4	0.40
Eof94	7	0.0	0.03
Eof94	8	0.5	1.14
Eof94	9	0.0	0.00
Eof94	10	-0.2	-0.07
Eof94	11	-0.1	-0.12

All eof magnitudes are within 3 standard deviations of mean

Eof14	1	-99.1	-0.36
Eof14	2	5.0	0.23
Eof14	3	-0.2	0.74
Eof14	4	-0.2	-0.02
Eof14	5	-2.5	-1.55
Eof14	6	-0.3	-0.87
Eof14	7	0.2	-1.09
Eof14	8	0.0	0.44
Eof14	9	-0.7	-0.88
Eof94	1	-5.7	-0.31
Eof94	2	5.3	**3.67**
Eof94	3	-1.4	-2.14
Eof94	4	0.0	-0.09
Eof94	5	0.6	0.79
Eof94	6	0.2	0.26
Eof94	7	-0.1	-0.23
Eof94	8	1.4	**3.31**
Eof94	9	4.3	**9.34**
Eof94	10	1.2	2.49
Eof94	11	-2.4	**-4.63**

4 eof magnitudes are > 3 standard deviations from their means

Eof14	1	-96.3	-0.22
Eof14	2	6.9	0.60
Eof14	3	3.7	2.81
Eof14	4	-1.8	-1.26
Eof14	5	0.2	1.09
Eof14	6	1.9	1.45
Eof14	7	2.5	1.77
Eof14	8	0.0	0.32
Eof14	9	0.3	0.68
Eof94	1	-2.7	0.59
Eof94	2	-1.4	-0.61
Eof94	3	0.7	0.50
Eof94	4	-0.4	-0.79
Eof94	5	-0.6	-1.10
Eof94	6	-0.0	-0.29
Eof94	7	0.4	0.84
Eof94	8	-2.3	**-5.49**
Eof94	9	-0.1	-0.38
Eof94	10	-0.8	-1.28
Eof94	11	-0.3	-0.66

One eof magnitude is > 3 standard deviations from its mean

⇒ To remove the multiple scattering once it is detected:

⇒ write equations requiring the last 3 (or the last 4, or the last 5, etc) principal components to be equal to their respective mean (which should cause a smaller error than the multiple scattering contribution), and solve these equations simultaneously for the lowest 3 (or 4, or 5, etc) corrected values of DZ_{94}

⇒ stability will depend on the determinant of that 3x3 (or 4x4 or 5x5 etc) matrix, and the error will depend on the magnitude of the inverse …

(use 9 Z_{14} and 11 ΔZ_{94} together)

To generate a global synthetic dataset:

1) Enforce consistency in the joint behavior of the DSD parameters with GV DSD data ➔

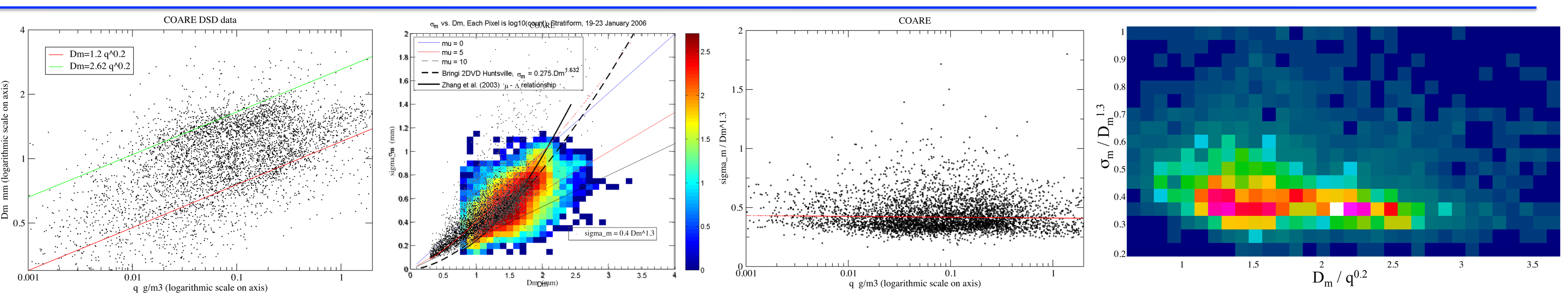

2) Using parameters $D_m / q^{0.2}$ and $\sigma_m / D_m^{1.3}$ retrieve underlying water contents consistent with 14 and 94 GHz Measurements, then

3) forward compute scattering signatures at the GPM active and passive frequencies

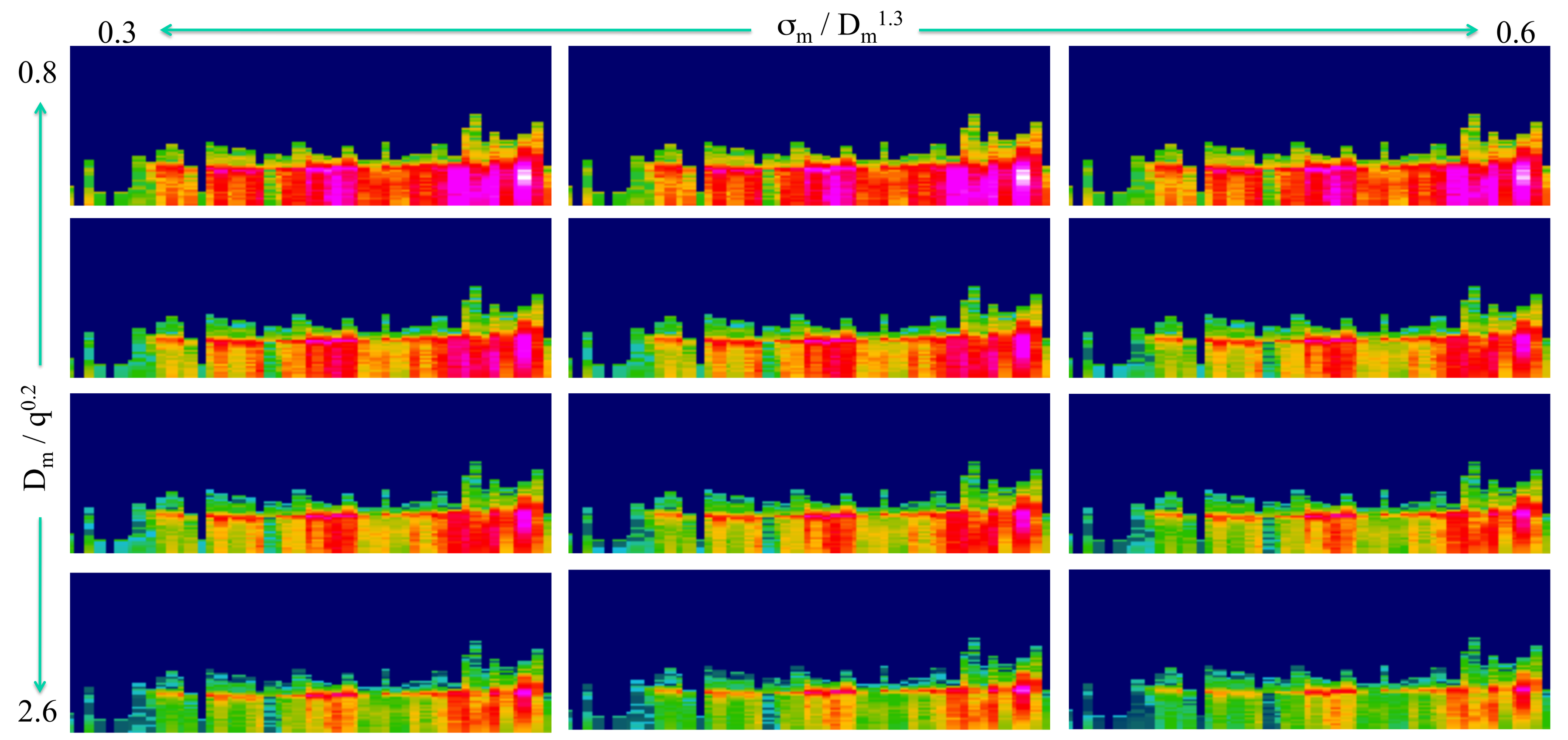

Wait!
…
There's more!

CloudSat + ground radar:

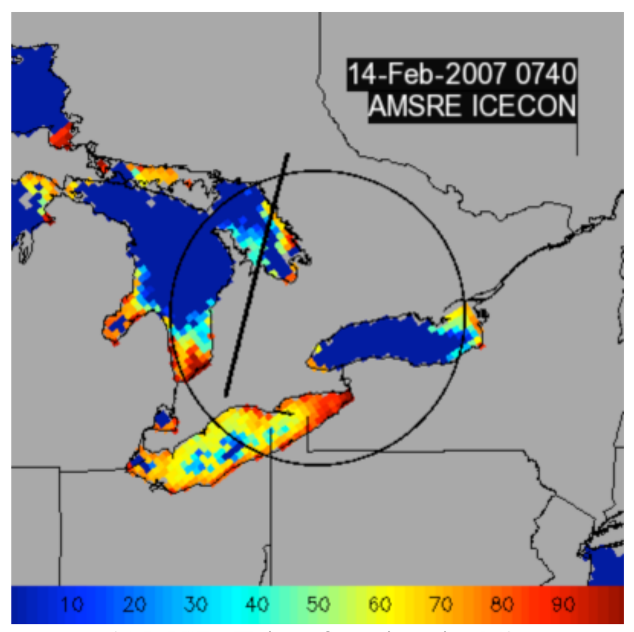

(AMSR-E ice fraction in %)

CloudSat descending pass thru WKR (King City) radar coverage

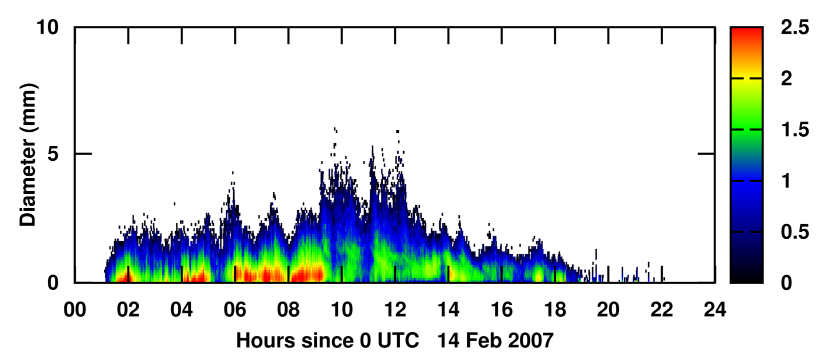

Co-located 2D-video DSD data (above) allows DSD parametrization (below)

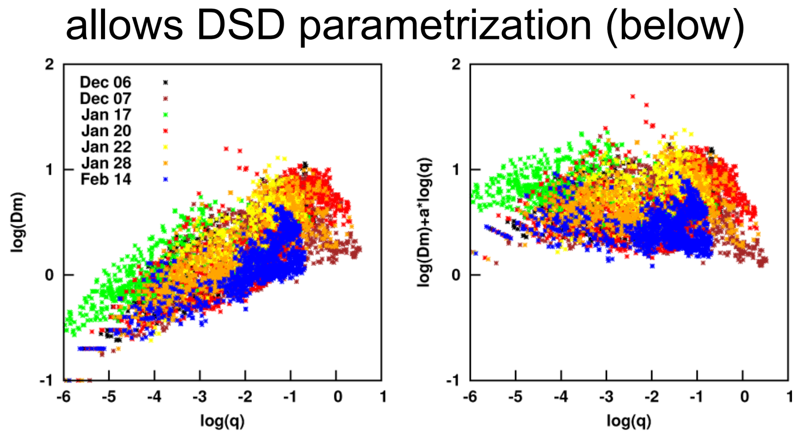

⇒ Retrieval of snow: